Kilovolt $^{33}S(n,\alpha_0)$ and $^{33}S(n,\gamma)$ cross sections: Importance in the nucleosynthesis of the rare nucleus ^{36}S†

G. F. Auchampaugh
Los Alamos Scientific Laboratory, Los Alamos, New Mexico 87544

J. Halperin
Chemistry Division, Oak Ridge National Laboratory, Oak Ridge, Tennessee 37830

R. L. Macklin
Physics Division, Oak Ridge National Laboratory, Oak Ridge, Tennessee 37830

W. M. Howard
Astronomy Department, University of Illinois, Urbana, Illinois 61801

(Received 24 March 1975)

The $^{33}S(n,\alpha_0)$ and $^{33}S(n,\gamma)$ cross sections have been measured from ~10 to ~700 keV. Resonance parameters are given for 39 resonances. The level spacing is determined to be 9.1±0.9 keV. The $\sigma(n,\alpha_0)$ and $\sigma(n,\gamma)$ cross sections are averaged over a Maxwellian distribution for values of kT from 25 to 275 keV. When these cross sections are used in a nucleosynthesis calculation of the rare isotope ^{36}S, the overproduction of this isotope, relative to the other nuclei formed in the universe, is reduced from a factor of 10 to 2.5.

[NUCLEAR REACTIONS $^{33}S(n,\alpha_0)$, $^{33}S(n,\gamma)$, $10<E_n<700$ keV; deduced A_γ, $\Gamma_\alpha/\Gamma_\gamma$, $\langle D\rangle$; Maxwellian averaged $\sigma(n,\alpha_0)$ and $\sigma(n,\gamma)$ for $kT<275$ keV.]

I. INTRODUCTION

The nucleosynthesis of many rare nuclei in our solar system from the interaction of seed nuclei with the free protons and neutrons liberated during the explosive burning in the cores of supernovae has been considered by Howard *et al.*[1] The parameters of the exploding gas (temperature, density, and free neutron-proton concentrations) as well as many reaction cross sections and nuclear binding energies are important in determining the abundances of these rare nuclei.

One isotope of special interest in this nucleosynthesis study is ^{36}S. It is produced by successive (n,γ) reactions on the primordial seed nucleus ^{32}S and by successive endothermic (n,p) reactions on the seed nucleus ^{36}Ar. Of particular importance in the first sequence is the branching ratio $\Gamma_\alpha/\Gamma_\gamma$ for the compound nucleus ^{34}S. A current calculation of this ratio of ≃22 by Truran[2] leads to an overproduction of ^{36}S relative to the other products formed in the explosive carbon-burning cycle by as much as a factor of 10. This branching ratio is also of importance in the astrophysical s process.

We have therefore undertaken measurements of the $\sigma(n,\gamma)$ and $\sigma(n,\alpha)$ cross sections of ^{33}S in the kilovolt neutron energy region at the Los Alamos Van de Graaff facility and at the Oak Ridge electron linear accelerator (ORELA).

II. $^{33}S(n,\alpha)$ MEASUREMENT

A. Experimental details

The $^{33}S(n,\alpha)$ cross section was measured relative to the ^{235}U fission cross section. The α particles and fission fragments were detected with silicon surface barrier detectors.

The Los Alamos Scientific Laboratory (LASL) vertical Van de Graaff accelerator was used to produce the sources of neutrons for the n,α measurements through the $^7Li(p,n)$ reaction. The proton beam was bunched to a pulse width of approximately 1 ns by a Mobley buncher at a rate of 2 MHz yielding average currents of the order of 1.5 μA.

Both lithium metal and lithium fluoride were used in fabricating the natural lithium targets. A thick lithium target with a proton energy loss of ~3 MeV was made by pressing lithium metal into a 0.25-mm-deep circular depression in a 1-mm-thick tantalum disk. A thinner lithium target with ΔE_p ~60 keV was made by evaporating lithium fluoride onto a 1-mm thick tantalum disk to an areal density of 0.50±0.05 mg/cm².

The thinner target was used to produce monoenergetic neutron beams for the neutron energy region from ~200 to ~700 keV. Data were taken at proton energies of 1.934, 2.019, 2.066, 2.114, 2.163, 2.213, 2.264, 2.316, 2.368, and 2.420 MeV. The calculated proton energy spread ΔE_p for a

$\frac{1}{2}$-mg/cm^2-thick LiF target is ~55 and ~65 keV for 2.42-MeV and 1.934-MeV protons, respectively. The energy resolution ΔE_n of the neutron spectra for these proton energies is approximately equal to ΔE_p except for the lowest energy. For the 1.934-MeV protons, $\Delta E_p > E_p - E_{th}$, where $E_{th} = 1.8811$ MeV,[3] the threshold for the ^{7}Li(p, n) reaction. Therefore, the neutron spectrum is characteristic of a thick lithium target and does not have a well-defined E_n.

The thick target was used to produce a continuous spectrum of neutrons for the energy region from 10 to 100 keV. Data were taken at proton energies of 2.2, 2.395, and 2.8 MeV. The neutron energy resolution of the thick target data was approximately three times better than that for the 1.934 MeV data.

The $^{33}S(n, \alpha)$ samples were prepared by the Isotope Division of Oak Ridge National Laboratory. The ^{33}S (91.81% isotopic enrichment) was evaporated onto 254-μm-thick 99.99% pure aluminum foils to an areal density of approximately 600 μg/cm^2. Four such samples were made with a total sulfur weight of 12.4 mg. The $^{235}UO_2$ (93%) and ^{10}B (96.5%) samples which were used to measure the neutron flux were made by electroplating the isotopes onto 25.4-μm-thick stainless steel foils to areal densities of 208.6 μg/cm^2 and 315 μg/cm^2, respectively. Both the sulfur and uranium deposits had equal areas. The foils were placed as close as possible to the front surfaces of the detectors for maximum particle detection efficiency.

The four 6-cm^2 silicon surface barrier detectors used in the experiment were placed on a circle of radius 3.5 cm. The distance from the lithium target to the center of each detector was 25.7 cm (7.8°) and 9.5 cm (21.6°) for the thick and thin target measurements, respectively. The number in parentheses gives the angle the detector made with respect to the proton beam direction. For the thin target measurements, two of the detectors viewed foils containing ^{33}S and one viewed a foil containing ^{235}U. The other detectors were not used in the thin target measurements. For the thick target measurements, all four detectors viewed ^{33}S foils. In addition, a 1-cm^2 detector was placed at the axis of the four larger detectors and viewed a foil containing ^{10}B. All detectors were enclosed in a hemispherical aluminum vacuum chamber with a dome wall thickness of 1.02 mm.

A schematic of the electronic setup is shown in Fig. 1. One Ortec-463 constant fraction discriminator (CFD) was used for all four ^{33}S detector systems. To achieve the best time resolution, it was important that the time delays between the initiation of a charged particle in a particular detector and the input to the EG&G TDC-100 time digitizer be the same for all four detectors. A pulsed semiconductor laser was used to measure these time delays. Appropriate length cables were inserted after each Tennelec TC-163 preamplifier to align all four detectors. The slow risetime of the signals (~100 ns) from the preamps due to the high capacitance of the large surface barrier detectors limited the over-all timing resolution for the four detectors to about 14 ns. Ortec-454 timing filter amplifiers with integration time constants of 100 ns were used to improve the uniformity of the pulses to the CFDs. The CFDs were modified to accept the slower risetime signals by providing for an external delay in the Ge(Li) mode of operation. The XDS-930 computer was set up to record both pulse height and time-of-flight (TOF) data simultaneously, but not in coincidence, at each proton energy. The TOF data from the uranium or boron and sulfur systems were routed into separate regions of the memory by tag bits and sorted into 2-ns time bins.

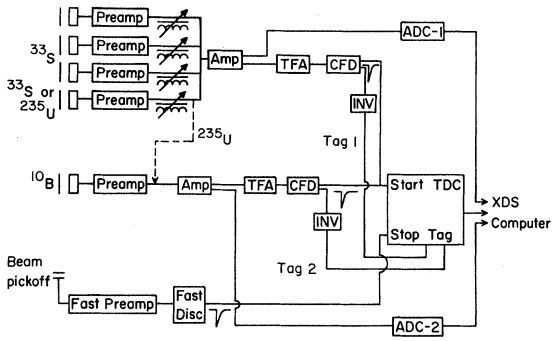

FIG. 1. Schematic of electronic setup.

B. Data reduction and results

1. Thin target

Chronologically, the data using the lithium fluoride target were taken after those with the lithium metal target. However, since some of the lithium fluoride data were used in the analysis of the thick target data, the reduction of the thin target data will be discussed first.

The $^{33}S(n, \alpha)$ cross section σ_α is related to the ^{235}U fission cross section σ_f by the simple relationship

$$\sigma_\alpha(E_n) = KC_s\sigma_f(E_n)/C_u \ , \tag{1}$$

where C_s = number of α particles detected from the ^{33}S in a given neutron energy bin, C_u = number of fission fragments detected from the ^{235}U in the same energy bin, and K is a normalization con-

stant which takes into account the relative sample masses and the target-sample-detector solid angles for the two detector systems. Since the detector systems were designed to have equal solid angles, K is just a ratio of the number of uranium atoms to sulfur atoms present in the samples.

An inspection of the sulfur foils prior to taking the thin target data revealed that much of the sulfur had disappeared from the foils. Therefore K could not be calculated from the sulfur weights supplied by ORNL and had to be measured.

The entire detector system was exposed to a uniform thermal neutron beam obtained from the thermal column at the LASL Omega West reactor. This measurement was made a few days after completing the thin target measurements.

Using 140 ± 30 mb [4] for $\sigma_{th}(n, \alpha_0) \sim \sigma_{th}(n, \alpha)$ of ^{33}S and 582.2 ± 1.3 b [4] for $\sigma_{th}(n, f)$ of ^{235}U in Eq. (1) results in a value of K of 0.082 ± 0.017, which corresponds to a sulfur weight of 1.74 mg, about one-third of the original weight for the two foils used in the thin target measurements. The uncertainty in K includes counting statistics (1%) and the uncertainty in the thermal cross section values (21.4%).

A rather high continuous background due to the neutron source was observed in the silicon detectors. This background had a maximum α pulse height of approximately 2.0 MeV, which was determined by placing a blank aluminum foil in front of one of the silicon detectors. C_s in Eq. (1) included all α counts above this bias with no correction applied for lost α particles with pulse heights less than 2.0 MeV. Because of the high positive Q (3.39 MeV) of the $^{33}S(n, \alpha_0)$ reaction leading to the ground state in ^{30}Si, this correction was taken to be negligible. This high bias also means that no information was obtained for the reaction leading to the first excited state in ^{30}Si at 2.23 MeV. The ^{235}U deposit was thin enough so that a clean separation existed between the background and fission pulse height distributions.

The ENDF/B-IV [5] evaluation of the ^{235}U fission cross section was used for σ_f in Eq. (1). The incident neutron energy E_n was calculated for a proton energy of $E_p - \frac{1}{2}\Delta E_p$ for $E_p \geq 2.019$ MeV. The 1.934 MeV data were not directly converted to cross section but were instead used in the analysis of the higher resolution thick target data which will be discussed in the next section.

2. *Thick target*

Small errors in the position of the zero channel in the sulfur TOF spectra, coupled with the short flight path of 25.7 cm, restricted the region of reliable data to neutron energies below 100 keV.

The analysis of the thick target data required knowing the neutron spectrum shape at 21.6° for a thick lithium target. Our attempt to measure the spectrum at 0° simultaneously with the thick target measurements using the ^{10}B detector system failed; it was not possible at all proton energies to cleanly separate out from the high background in the silicon detector the low energy α_0 and α_1 groups from the ^{10}B reactions. We then compared the measured neutron spectrum at 7.8° (1.934 MeV) to a calculated spectrum at the same angle and found that the two spectra agreed to within 10% over the energy region from 25 to 100 keV. However, below 25 keV the calculated shape decreased more rapidly with decreasing neutron energy than the experimental shape and at 10 keV was about a factor of 2 lower. This difference was attributed to a room return neutron background in the data. The small differences between the calculated spectra at 7.8 and 21.6° were within the statistical errors on the experimental data points. Therefore, we used the measured neutron spectrum for the energy region from 25 to 100 keV, because it included the Al transmission dips from the Al vacuum chamber window, and used the calculated spectrum (7.8°) for the energy region below 25 keV.

Since the shape of the three sulfur TOF spectra should be independent of the proton energy below 100 keV neutron energy, they were summed together to improve the statistical accuracy of the data in this region. The sulfur TOF spectrum was then averaged over three channels and converted to a cross section using Eq. (1) with $K = 0.081 \pm 0.018$. The constant K was determined by requiring that the sum of the α counts for neutron energies below 128 keV (neutron energy corresponding to $E_p = 1.934$ MeV) be the same for the thick and thin (1.934 MeV) sulfur TOF spectra. The energy per channel difference between the two measurements, which is equal to the ratio of the two flight paths, is also included in K. The uncertainty in K includes the uncertainty in the thermal cross section values (21.4%), an uncertainty in flight paths (6%) and an uncertainty in the normalization of the two sets of data (5%).

3. *Results*

The final results from the combined thin (●) and thick (▲) target measurement data are shown in Fig. 2. The pronounced maxima in the cross section at 14 and 25 keV correspond to isolated resonances seen at these energies in the high resolution n, γ cross section reported herein. The broad maximum centered at about 65 keV corresponds to an envelope of approximately seven resonances. Sta-

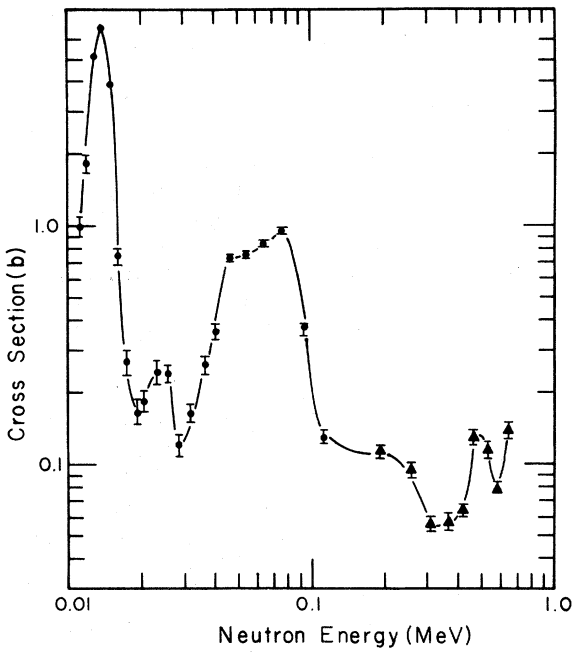

FIG. 2. The $^{33}S(n,\alpha_0)^{30}Si$ cross section from 10 to 650 keV. The data represented by the solid dots were taken with a white neutron source and those represented by solid triangles were taken with a monoenergetic neutron source. Statistical errors are plotted for those points with errors greater than the point size. The absolute error (relative error) in the cross section is 21.4% (5%) for $E_n > 200$ keV and 22.8% (10%) for $E_n < 100$ keV.

tistical errors are plotted for those points with errors greater than the point size. The absolute error (relative error) in the cross section is 21.4% (5%) for $E_n > 200$ keV and 22.8% (10%) for $E_n < 100$ keV.

III. $^{33}S(n,\gamma)$ MEASUREMENT

A. Experimental details

The Oak Ridge Electron Linear Accelerator was used to produce the neutrons for the n, γ measurement. Details of the characteristics of this facility, the experimental procedure, and associated electronics for n, γ measurements can be found in a number of references.[6,7] Consequently, only the details of the system pertinent to the present measurement are given in this section.

The 40-m capture facility at ORELA was used for neutron radiative capture measurements with the linac operating at power levels up to 17 kW for 5-ns pulses at a repetition rate of 1000 pulses per second. Two fluorocarbon liquid scintillators (Ne-226),[8] each 4-cm thick by 10-cm diameter, were mounted on 12.7-cm photomultipliers and viewed the capture sample normal to the beam. The application of a computed pulse-height weighting scheme to the output from these detectors resulted in an average response proportional only to the total energy (i.e., binding energy plus center-of-mass neutron energy). These detectors were referred to as total energy detectors (TED). They have an efficiency per capture of approximately 15% and a time resolution of less than 2 ns. The resulting over-all energy resolution (in keV) of the system was $1.67\times10^{-3}E_n$ at 20 keV to $3.34\times10^{-3}E_n$ at 750 keV. The incident neutron flux was monitored by a $\frac{1}{2}$-mm-thick ^{6}Li glass detector, viewed end-on by two photomultipliers 43 cm in front of the sample.

The data were stored in a SEL 810B computer with fast access disk storage in four disk files containing the ^{6}Li TOF spectrum, the TED TOF vs pulse-height matrix, the TED energy-weighted TOF spectrum, and the variance of this energy-weighted spectrum.

The ^{33}S sample (a disk 1.3-cm diameter by 0.4-cm thick) contained 1.089 g of sulfur with the following percent isotopic enrichments: $^{33}S = 88.21 \pm 0.08$, $^{32}S = 10.96 \pm 0.08$, $^{34}S = 0.81 \pm 0.02$, $^{36}S = 0.01$, giving a sample thickness of 0.0132 atoms/b for ^{33}S.

B. Data reduction and analysis

At the completion of the capture measurement, the data were dumped onto magnetic tape for off-line reduction and analysis at the IBM 360/91 computer. The data were corrected for dead-time, time-independent, and nonresonant time-dependent background. The total background subtraction was typically 8 or 9%. In addition to the nonresonant scattering background from the sample, there was also a γ yield associated with each resonance, derived from neutrons scattered at the sample resonance and subsequently captured in the detector or housing. This scattered neutron sensitivity expressed as a capture width was typically a few parts in ten thousand that of the neutron width.[9]

The time-of-flight spectra were converted to 12 linear energy groups from 2.5 keV to 2.5 MeV by an interpolative procedure, and then normalized to the ^{6}Li(n, α) cross section. The formalism given in Ref. 10 was used to calculate the ^{6}Li(n, α) cross section, with an additional resonance term at 2 MeV to fit the data above the 0.25-MeV p-wave resonance. The final result uncorrected for multiple scattering and self-shielding is shown in Fig. 3.

Resonance parameters were extracted for the resolved resonances by an automatic Gaussian fitting computer code. The output from this code was used in calculating resonance energies, widths,

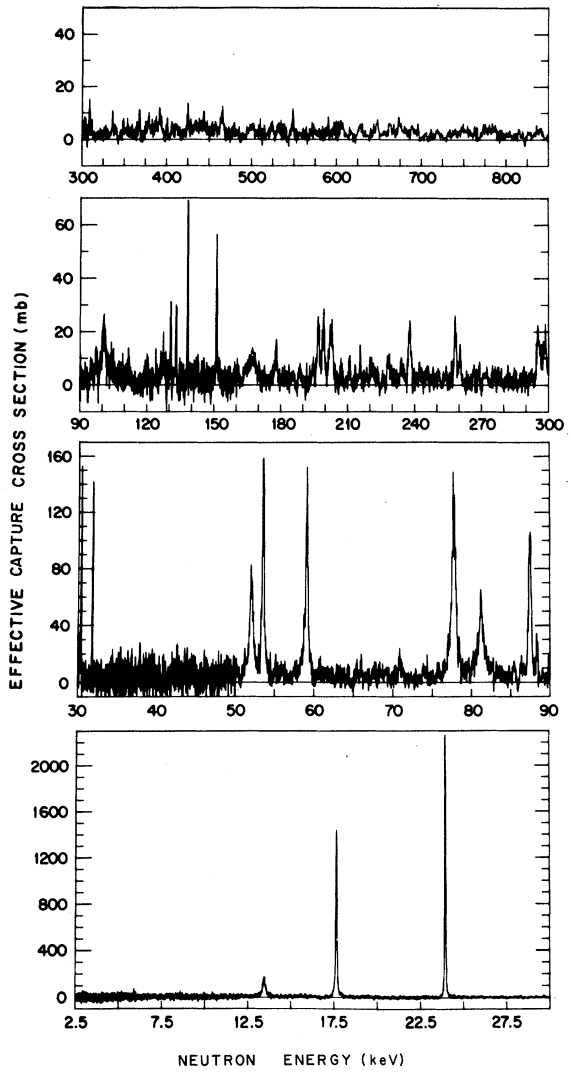

FIG. 3. The effective neutron capture cross section of $^{33}S(n, \gamma)^{34}S$ from 2.5 to 850 keV. The onset of γ rays produced by inelastic neutron scattering takes place just above 850 keV. Energy resolution is $E_n/600$ at 20 keV and falls to $E_n/300$ at 750 keV.

and capture areas relative to the $^6Li(n, \alpha)$ cross section. For most of the isolated resonances in ^{33}S, the observed width Γ_{obs} is much greater than the experimental resolution, and therefore it is possible to obtain directly an estimate of $g\Gamma_\gamma$. For these cases, assuming $\Gamma_n \sim \Gamma = \Gamma_{obs}$ and using the thin sample approximation, $g\Gamma_\gamma \cong A_\gamma/2\pi^2\lambda^2$. Using these estimates of Γ_n and Γ_γ, self-shielding and multiple scattering corrections were calculated and applied to the capture areas. These corrections are less than 10%, except for the three lowest energy resonances where the corrections are 20 to 30%. If Γ_{obs} was comparable to or less than the experimental resolution, then $g\Gamma_n\Gamma_\gamma/\Gamma$ only was obtained from the area analysis. Approximate corrections were made to the capture areas in this case, since insufficient data were available to evaluate Γ_n and Γ_γ individually.

IV. RESONANCE PARAMETERS

The resonance parameters obtained from the area analysis of the observed resolved resonances are presented in Table I. The total widths are obtained from a Gaussian fit to the resonances, folding in the experimental resolution and Doppler broadening, and not from a more exact Breit-Wigner[11] shape fit. A 20% error has been assigned to each Γ to account for this effect, as well as the multiple scattering and self-shielding corrections. A lower limit to $\langle g\Gamma_\gamma \rangle$ of about 1 eV or to $\langle \Gamma_\gamma \rangle$ of about 2 eV is obtained by assuming $\Gamma_n = \Gamma$ for all resonances given in Table I. In the next section $\langle \Gamma_\alpha/\Gamma_\gamma \rangle$ is shown to be about 90, which means that $\langle \Gamma_\alpha \rangle \sim 170$ eV. The Γ_α are expected to obey a χ^2 distribution of approximately 1 degree of freedom and, therefore, for many resonances the assumption $\Gamma_n \sim \Gamma$ is not correct. For this reason, only the capture areas are given in Table I.

The s-wave resonances are assigned by observing the interference minima in the ^{33}S total cross-section data of Good *et al.*[12] The ground state of ^{30}Si has a $I^\pi = 0^+$. The possible compound states in ^{24}S which undergo α decay to this state have $J^\pi = 0^+$, 1^-, 2^+, etc. The states formed by s-wave or p-wave neutron capture in ^{33}S are 1^+, 2^+, and 0^-, 1^-, 2^-, 3^-, respectively. Therefore all s-wave resonances seen in the n, α_0 cross section are 2^+ states and all p-wave resonances seen are either 1^- or 3^- states.

A cumulative distribution of the number of resonances observed in the interval from 13 to 240 keV above a neutron energy E_n yields for the value of the average level spacing, $\langle D \rangle$, 9.1 ± 0.9 keV. Above 250 keV resonances are missed or groups of resonances not completely resolved. The error is based on the Wigner surmise[13] for statistically independent level spacings. The resonance integral $\int \sigma dE/E$ above the cadmium cutoff is calculated to be 33.4 mb.

Our results can be compared at least qualitatively with those from the paper of Wiechers, McMurray, and Van Heerdon.[14] They measure the neutron and γ yield from the inverse reaction $^{30}Si(\alpha, n \text{ or } \gamma)$ as a function of α energy. The two resonances which can be compared are the ones at 13.4 and 23.9 keV. They observe no γ strength for the 13.4-keV resonance, but a very large neutron strength. Our ratio of $\Gamma_\alpha/\Gamma_\gamma$ of 370 supports

TABLE I. Resonance parameters for neutron capture in $^{33}S(n,\gamma)^{34}S$.

E_n (keV)	$\frac{g\Gamma_\gamma\Gamma_n}{\Gamma_{tot}}$ (eV)	Γ_{tot} (eV)	Comments
13.45	0.087± 0.006	107 ± 20	$l=0$ [a], $J=2^+$, $\Gamma_\alpha/\Gamma_\gamma \simeq 370$
17.62	0.556± 0.032	48.7± 9.7	
23.93	1.03 ± 0.055	46.1± 9.2	$\Gamma_\alpha/\Gamma_\gamma \simeq 4$
31.79	0.063± 0.004	<15 eV [b]	
52.00	0.314± 0.020	330 ± 70	$l=0$ [a], $J=2^+$
53.51	0.551± 0.033	240 ± 50	
59.07	0.674± 0.041	340 ± 70	
77.74	1.33 ± 0.08	480 ± 100	
81.19	0.59 ± 0.04	580 ± 120	$l=0$ [a], $J=2^+$
87.45	0.77 ± 0.05	240 ± 50	
88.32	0.139± 0.01	260 ± 50	
100.7	0.94 ± 0.08	1580 ± 300	
127.5	0.30 ± 0.04	850 ± 170	
130.6	0.34 ± 0.04	200 ± 40	
133.1	0.42 ± 0.03	230 ± 40	
138.2	0.92 ± 0.07	150 ± 30	
151.2	0.86 ± 0.07	340 ± 70	
167.0	1.67 ± 0.16	3300 ± 400	
177.6	0.55 ± 0.07	760 ± 150	
196.6	1.18 ± 0.10	710 ± 140	
199.1	1.09 ± 0.11	700 ± 140	
202.4	1.92 ± 0.15	1130 ± 200	$l=0$ [a], $J=2^+$
210.8	0.30 ± 0.05	310 ± 60	
215.6	0.32 ± 0.05	<120 eV [b]	
221.2	0.73 ± 0.11	1570 ± 300	$l=0$ [a], $J=2^+$
228.2	0.57 ± 0.08	630 ± 130	
237.5	1.60 ± 0.14	610 ± 120	
258.0	1.50 ± 0.12	400 ± 80	$l=0$ [a], $J=2^+$
260.2	0.81 ± 0.09	550 ± 110	
295.4	2.05 ± 0.16	610 ± 120	
298.2	1.92 ± 0.16	790 ± 160	
308.7	1.20 ± 0.22	670 ± 140	
335.9	0.70 ± 0.13	280 ± 60	
367.4	1.26 ± 0.18	400 ± 80	
377.9	2.77 ± 0.47	1400 ± 250	
391.3	3.06 ± 0.38	1300 ± 250	
425.3	1.43 ± 0.22	1700 ± 300	
465.4	3.18 ± 0.33	3300 ± 500	
548.4	2.77 ± 0.40	2300 ± 400	

[a] We are indebted to Good for allowing us to examine some preliminary transmission data.
[b] Resonance narrower than resolution.

their findings. For the 23.9-keV resonance, just the opposite is observed in their data, which again is in reasonable agreement with our ratio of $\Gamma_\alpha/\Gamma_\gamma$ of 4.0. The poor resolution of our n,α measurement prevents drawing any further correlation for the higher energy resonances.

V. MAXWELLIAN-AVERAGED SECTIONS

Of interest to the astrophysicist in nucleosynthesis calculations is the nuclear cross section thermally averaged over a Maxwellian distribution of interacting particles as a function of energy. For neutron-induced reactions, the relevant energy range is from 30 to about 500 keV. For example, in the quiescent s process, or multiple neutron capture on a time scale slow compared with β decay lifetimes, the kinetic energy is the order of 30 keV, while for explosive nucleosynthesis processes the energy range of interest is from 100 to 500 keV.

The Maxwellian average cross sections are given in Fig. 4 for values of kT between 25 and 275 keV. $\langle\sigma_\gamma V\rangle V_T$ is calculated from the formula given in Ref. 15 using the resonance parameters in Table I and assuming a thermal value of 20 mb[4] for $\sigma(n,\gamma)$. Calculating the average in this way from the resonance parameters eliminates some of the problems associated with correcting the effective capture cross section for multiple scattering and self-shielding effects. The absolute error on this curve is approximately 10%. $\langle\sigma_\alpha V\rangle V_T$ is calculated by folding the Maxwellian distribution into the measured (n,σ) cross section and evaluating the integral numerically with the trapezoidal rule from thermal energy to 800 keV, with the cross section at 800 keV equal to that at the last measured data point. The absolute error on this curve is approximately 25%. $\langle\sigma_\alpha/\sigma_\gamma\rangle$ is approximated by $\langle\sigma_\alpha\rangle/\langle\sigma_\gamma\rangle$ because of the large differences in the energy resolutions of the two measurements and the difficulty of aligning the two sets of data over isolated resonances.

As a convenience to the nuclear astrophysicist, we present the quantity $N_A\langle\sigma V\rangle$ as a function of

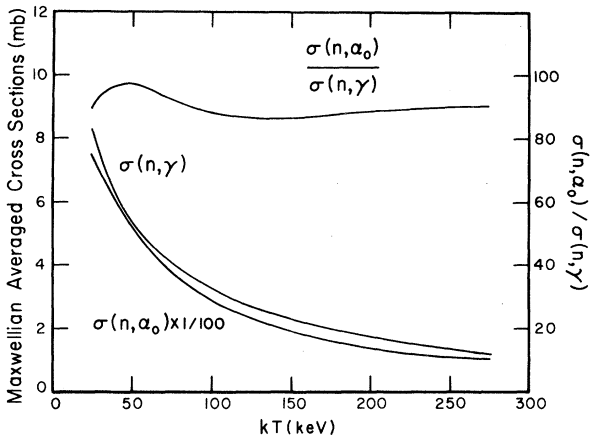

FIG. 4. Maxwellian-averaged $^{33}S(n,\alpha_0)^{30}Si$ and $^{33}S(n,\gamma)^{34}S$ cross sections and the ratio of these averaged cross sections for values of kT between 25 and 275 keV. The absolute error in the Maxwellian-averaged cross sections is 25% for $\sigma(n,\alpha_0)$ and 10% for $\sigma(n,\gamma)$.

kinetic temperature $T_9(10^9\,\mathrm{K})$.

$$N_A\langle\sigma_\gamma V\rangle = \exp(9.972 + 7.372/T_9^{1/3} - 4.483/T_9^{2/3} + 0.871/T_9)$$

and

$$N_A\langle\sigma_\gamma V\rangle = \exp(14.366 + 7.494/T_9^{1/3} - 4.321/T_9^{2/3} + 0.750/T_9)\,,$$

where N_A is Avagodro's number. These expressions reproduce the Maxwellian average data within about 6.5% over the temperature range $0.3 \lesssim T_9 \lesssim 3.0$.

Only the n, α cross section leading to the ground state ($I^\pi = 0^+$) in ^{30}Si has been measured. However, the contribution to the total (n, α) cross section for deexcitation to the first excited state ($E_{ex} = 2.23$ MeV, $J^\pi = 2^+$) in ^{30}Si is completely negligible. A hindrance factor of approximately 10^{-9} is calculated considering only the difference in energy between the ground state and the first excited state.

VI. IMPORTANCE OF ^{33}S(n,γ) AND ^{33}S(n,α) TO NUCLEAR ASTROPHYSICS

To have a viable theory for the origin of the natural elements, it is important to account for the existence of all the naturally occurring nuclei, no matter how small their abundance. The rare neutron-rich isotope ^{36}S is thought to be formed from the conversion of ^{32}S and ^{36}Ar, initially present in the star during explosive carbon burning. However, if all of the ^{32}S and ^{36}Ar initially present is converted into ^{36}S, the ^{36}S is overproduced relative to the other products of explosive carbon burning by a factor of 100. Thus, the reaction sequences leading from ^{32}S and ^{36}Ar must finely regulate the amount of ^{36}S produced.

The following are the important reaction sequences:

(1) $^{36}\mathrm{Ar}(n, p)^{36}\mathrm{Cl}(n, p)^{36}\mathrm{S}$

and

(2) $^{32}\mathrm{S}(n, \gamma)^{33}\mathrm{S}(n, \gamma)^{34}\mathrm{S}(n, \gamma)^{35}\mathrm{S}(n, \gamma)^{36}\mathrm{S}$, with ^{37}Cl, (p, α), (p, γ), (n, α), ^{30}Si

When the rates used in these sequences are based on the optical model calculations by Truran,[2] ^{36}S is overproduced by as much as a factor of 10. When the measured cross sections reported here are used, this overproduction can be reduced to a factor of 2.5. The problem still contains many nuclear uncertainties that have an important bearing upon the results, however. The interested reader is referred to papers by Howard *et al.*,[1] Clayton and Woosley,[16] and Fowler, Caughlan, and Zimmerman[17] for many nuclear details for which accurate laboratory measurements are needed to confirm or constrain many of the ideas about the origin of the elements.

ACKNOWLEDGMENT

We are indebted to R. R. Winters of Denison University for much of the programming used in the analysis of the capture data, and to W. M. Good of ORNL for allowing us to examine some preliminary transmission data. One of us (W. M. H.) would like to acknowledge the support by the National Science Foundation Grant No. MPS 73-0511-7.

---

†Work done under the auspices of the U.S. Energy Research and Development Administration.

[1]W. M. Howard, W. D. Arnett, D. D. Clayton, and S. E. Woosley, Astrophys. J. 175, 201 (1972).
[2]J. W. Truran, Astrophys. J. 18, 306 (1972).
[3]See J. H. Gibbons and H. W. Hewson, *Fast Neutron Physics*, edited by J. B. Marion and J. L. Fowler, (Interscience, New York, 1960), Chap. I.E.
[4]*Neutron Cross Sections*, compiled by S. F. Mughabghab and D. I. Garber, Brookhaven National Laboratory No. BNL-325 (National Technical Information Service, 1973), 3rd ed., Vol. I, Resonance Parameters.
[5]ENDF/B-IV, MAT1261, tape distributed by Brookhaven National Laboratory in 1974.
[6]B. J. Allen, R. L. Macklin, R. R. Winters, and C. Y. Fu; Phys. Rev. C 8, 1504 (1973).
[7]R. L. Macklin and J. H. Gibbons, Phys. Rev. 159, 1007 (1967).
[8]Nuclear Enterprises, Inc., San Carlos, California 90063.
[9]B. J. Allen and R. L. Macklin, Phys. Rev. C 3, 1737 (1971).
[10]R. L. Macklin, J. Halperin, and R. R. Winters, Phys. Rev. C 11, 1270 (1975).
[11]G. Breit and E. P. Wigner, Phys. Rev. 49, 519 (1936).
[12]W. M. Good (private communication).
[13]E. P. Wigner, in Proceedings of the Conference on Neutron Physics by Time-of-Flight, Gatlinburg, Tennessee, 1956 [Oak Ridge National Laboratory Report No. ORNL-2309, 1956 (unpublished)], p. 59.

[14]G. Wiechers, W. R. McMurray, and I. J. Van Heerdon, Nucl. Phys. A92, 175 (1967).
[15]R. L. Macklin and J. H. Gibbons, Rev. Mod. Phys. 37, 166 (1965).
[16]D. D. Clayton and S. E. Woosley, Rev. Mod. Phys. 46, 755 (1974).
[17]W. A. Fowler, G. R. Caughlan, and B. A. Zimmerman, Annu. Rev. Astron. Astrophys. 13, 69 (1975).